



Influence of collars on reduction in scour depth at two piers in a tandem configuration

Sargol Memar^{1,2} · Mohammad Zounemat-Kermani¹ · Aliasghar Beheshti³ · Majid Rahimpour¹ · Giovanni De Cesare² · Anton J. Schleiss²

Received: 2 September 2019 / Accepted: 6 December 2019 / Published online: 11 December 2019
© Institute of Geophysics, Polish Academy of Sciences & Polish Academy of Sciences 2019

Abstract

Bridge failure, due to local scour at bridge pier foundations, has become a critical issue in river and bridge engineering, which might lead to transportation disruption, loss of lives and economic problems. A practical solution to prevent bridge collapses is the implementation of scour mitigation methods around bridge foundations. Based on an experimental perspective, this study is focused on the influence of the size and position of circular collars from the sediment bed on scour depth at two tandem piers. To meet this end, long-lasting experiments are performed under clear-water conditions using uniform sand for bed materials. Compared to the adjacent position of the collar on the bed, placing the collars below the bed would increase the delay time of scour at the piers up to four times. However, regardless of the delay time, the observations indicate that locating the collars on the initial bed surface results in maximum reduction in scour depths around the piers. It was found that diminishing the flow intensity has a dramatic impact on the scour reduction at the piers, so that maximum reduction in scour depths at piers increased on average from 20 to 70% with the reduction in the flow intensity from 0.95 to 0.9.

Keywords Bridge foundation · Collar · Countermeasure · Horseshoe vortex · Scour depth reduction

List of symbols

B	Width of the channel
D	Pier diameter
D^*	Equivalent pier width
D_{proj}	Sum of the non-overlapping projected width of the piers onto a plane normal to the flow direction
d_s	Depth of scour
d_{se}	Equilibrium depth of scour
$d_{\text{s(ext)}}$	Extrapolated depth of scour to an infinite time
d_{50}	Median sediment grain size
g	Acceleration of gravity
h	Upstream flow depth
H_c	Collar height from the sediment bed

K_m	Number of aligned rows factor
K_{sp}	Factor for the distance between the piers
R	Reduction in scour depth
R_u	Reduction in scour depth at the upstream pier
R_d	Reduction in scour depth at the downstream pier
$R_p = UD/\vartheta$	Pier Reynolds number
s	Center-to-center spacing of the piers
U	Mean upstream flow velocity
U_c	Mean threshold velocity
u_c^*	Shear critical velocity
T	Dimensionless time of scour
t	Time of scour
t_c	Thickness of the collar
t_d	Delay time of scour
t_e	Equilibrium time of scour
w_c	Width of the collar
Z	Dimensionless scour depth
$\Delta = \rho'_s/\rho$	Relative submerged sediment density
ϑ	Fluid kinematic viscosity
ρ	Density of fluid
ρ_s	Sediment grain density
ρ'_s	Submerged sediment density

✉ Mohammad Zounemat-Kermani
zounemat@uk.ac.ir

¹ Department of Water Engineering, Shahid Bahonar University of Kerman, Kerman, Iran

² Laboratory of Hydraulic Constructions, Ecole Polytechnique Fédérale de Lausanne, Lausanne 1015, Switzerland

³ Department of Water Engineering, Ferdowsi University of Mashhad, Mashhad, Iran

σ_g	Geometric standard deviation of the sediment grain size distribution
φ	Function

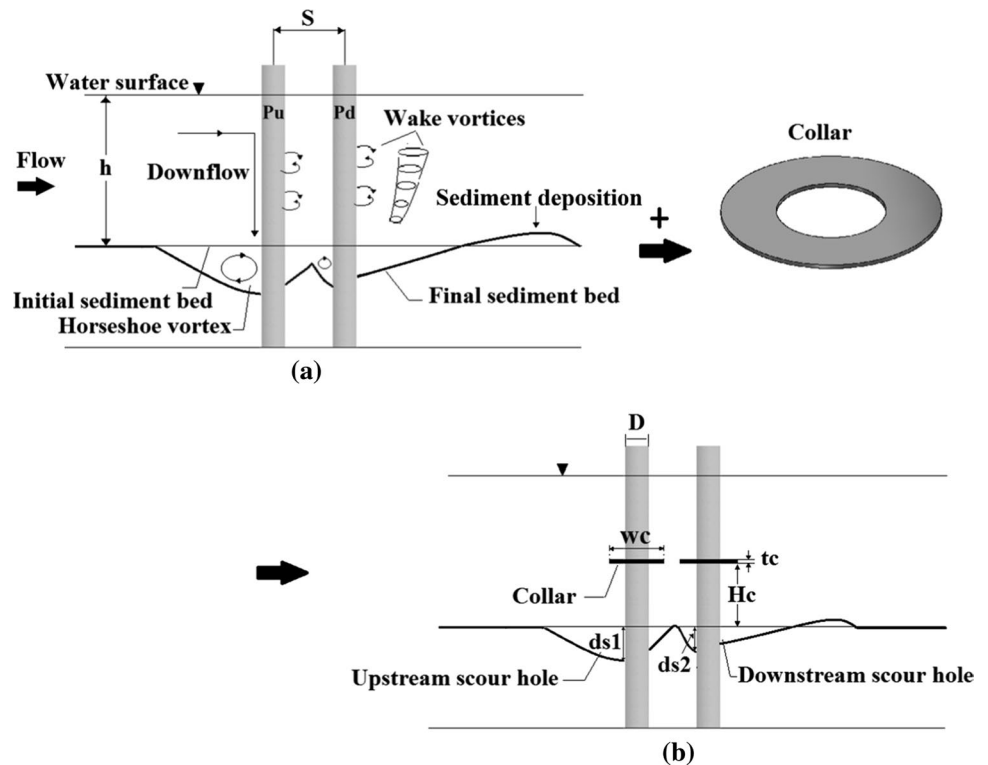
Introduction

Local scour at bridge foundations (piers and abutments) can be a significant hazard causing instability or collapse of such vital infrastructures. Pier scour is described as an erosion that undermines the bridge foundations. The erosive effect of flowing water forms bridge scour by the excavation and removal of sediment grains from around the abutments and piers of the bridges. Prediction of the depth of scour around bridge foundations is a fundamental part of designing safe bridges. Scour monitoring at bridges is performed regularly to maintain bridge safety against scour-induced failure (Ettema et al. 2006). In order to better understand the scour at the piers, it is of paramount importance to understand the flow pattern and performance of the large-scale coherent structures that are formed around the piers. In Fig. 1a, pier scour is depicted around two tandem piers. The approach flow velocity accelerates at the upstream of the piers and the flow is directed toward the sediment bed on the front face of the piers, which is called downflow. Where the downflow reaches the sediment bed, the horseshoe vortices are formed. Generally, scour begins at the flanks of the pier. Once the scour area extends as a hole around the pier, the

downflow and horseshoe vortices are strengthened, resulting in the development of the scour hole around the pier. By separating the approach flow from the sides of the piers, vortex shedding is generated in the piers' wake (Raudkivi 1986; Arneson et al. 2012 (HEC-18); Guo et al. 2012). In the case of two tandem piers, the existence of the upstream pier causes a reduction in the amount of the approach flow velocity toward the downstream pier. Thus, the rate of scour around the downstream pier is less than that around the upstream pier. When the scour holes around the piers overlap, the movement of sediment particles from upstream is facilitated, leading to increasing the depth of scour at the upstream pier (Hannah 1978; Lança et al. 2013). The variables P_u and P_d indicate the upstream and downstream piers, respectively.

Scour at bridge piers may occur under clear-water or live-bed scour conditions. According to Melville (1984) and Chiew (1984), the scour depth achieves two peaks depending on flow intensity. The first peak is called clear-water threshold peak and the second peak is termed as the live-bed peak. Under clear-water conditions and with uniform sediments, the scour depth increases approximately linearly with flow intensity and achieves its maximum value at the onset of sediment movement (at threshold velocity). The maximum scour depth is called threshold peak. Once the mean upstream flow velocity exceeds the threshold velocity, the scour depth reduces in the relatively small conversion of flow intensity and, then, increases again reaching the

Fig. 1 Schema of the flow field and scour holes around two tandem piers: **a** without collars; **b** with collars above the sediment bed, (d_s scour depth, h upstream flow depth, H_c collar height from the sediment bed, w_c width of the collar, t_c thickness of the collar, s center-to-center spacing of the piers, D diameter of the pier)



live-bed peak, leading to the formation of bedforms. Bedforms transport into the scour hole periodically, resulting in the periodic variation of maximum scour depth. In clear-water scour conditions, no upcoming sediment grain enters the scour hole (Shen et al. 1966; Ettema 1980; Melville and Chiew 1999; Sheppard and Miller (2006)).

Several methods have been examined for scour depth estimation at bridge piers by many investigators (Dey 1997a, b; Oliveto and Hager 2002, 2005; Zounemat-Kermani et al. 2009; Arneson et al. 2012; Sheppard et al. 2013; Pang et al. 2016). Many efforts have been made by researchers to reduce the dimensions of scour holes around the piers using several scour countermeasures. The choice of a proper pier countermeasure for a particular bridge is based on the flow conditions and features of the nearby channel (Johnson et al. 2002). There are two different types of scour countermeasures. Countermeasures such as bed sill, submerged vane and collar deflect the approach flow and minimize the power of the system of vortices around the pier, resulting in the reduction in scour depth. Other scour countermeasures are placed on the sediment bed to protect it from erosive and hydraulic forces consisting of riprap stones, cable-tied blocks and geobags (Tafarojnoruz et al. 2012; Khaple et al. 2017a).

Collars are thin horizontal disks that are attached around a pier (see Fig. 1). The collars protect the sediment bed from erosion caused by the downflow and horseshoe vortices. Thus, they reduce the scour potential around the pier. The effect of collars on scour depth at isolated bridge piers has been studied by several investigators (Kumar et al. 1999; Zarrati et al. 2004; Moncada-M et al. 2009; Masjedi et al. 2010; Tafarojnoruz et al. 2012;

Zokaei et al. 2013; Khodashenas et al. 2018; Karimaei Tabarestani and Zarrati, 2019). However, limited research has reported the influence of collars on scour reduction around the pier groups. Zarrati et al. (2006) examined the effect of the collars placed on the sediment bed on scour depths at two side-by-side and tandem piers. Heidarpour et al. (2010) studied the influence of collars on scour depth reduction at two and three tandem piers when the collars were set on the original bed. Figure 1b schematically illustrates scour holes around two tandem piers equipped with collars. Parameters d_{s1} and d_{s2} refer to scour depth at the upstream and downstream piers, respectively. Table 1 presents a summary of the essential experimental studies on the effect of collars on scour at the piers along with the obtained percentage reduction at scour depth in each study (the last column).

The effect of collars on scour depth at bridge piers is assessed based on the width of collar w_c and the collar height from sediment bed H_c . According to Table 1, the collar's effectiveness in reducing the scour depth around the pier increases with increasing the width of the collar. However, a collar that is wider than three times of the pier diameter is not applicable in practice (Zarrati et al. 2006). In addition, the optimal height of collars that results in maximum scour depth reduction around the piers depends on different factors of experimental condition, pier skewness and pier shape.

Furthermore, in most of the previous studies, the experiments have been performed for short durations of scour (e.g., 7 h), in which the equilibrium depth of scour has not been achieved. Given that the scour at bridge piers

Table 1 Experimental studies using collars against scouring at bridge piers (w_c width of the collar, D pier width or diameter, H_c collar height from the sediment bed, h upstream flow depth)

Authors	No. piers	Pier shape	Collar shape	w_c/D	H_c/h	Maximum reduction in scour depth (%)
Zarrati et al. (2004)	1	Rectangular rounded nose	Rectangular rounded nose	2, 3	From $0.4D$ to $-0.8D^a$	74 for: $w_c/D = 3$ (on the sediment bed)
Zarrati et al. (2006)	2	Circular	Circular independent and continues	3	0	30 (first pier) 75 (second pier)
Moncada-M et al. (2009)	1	Circular	Circular	2, 3	$0, \pm 3, \pm 6, \pm 9$	100 (for: $w_c/D = 3$, on the sediment bed) 96 (for: $w_c/D = 2$, on the sediment bed)
Masjedi et al. (2010)	1	Oblong	Oblong	1, 1.5, 2, 2.5, 3	$0, -0.1D, -0.5D, -1D$	92 (for: $w_c/D = 3$ and $H_c/D = -0.1$)
Heidarpour et al. (2010)	2, 3	Circular	Circular	2, 3	0	45 (third pier of three tandem piers) 44 (second pier of two tandem piers)
Tafarojnoruz et al. (2012)	1	Circular	Circular	3	0	28.7
Chen et al. (2018)	1	Circular	Hooked	1.25	0, 0.25	42 (on the sediment bed)

^aNote The negative values of H_c/h are corresponding to the collar height below the sediment bed

increases over time until the equilibrium condition is achieved, it is necessary to assess the effect of collars on scour reduction at the equilibrium time.

Zarrati et al. (2004) showed that the maximum scour depth reduction at a rectangular nose pier was obtained when the collar was placed on the sediment bed. In contrast Kumar et al. (1999) found that lowering the collar below the bed led to less scour at the pier, followed by increasing the dimensions of the scour hole compared to the case where the collar was positioned on the bed. Masjedi et al. (2010) indicated that, at an oblong pier situated in a 180° channel bend, locating the collar under the sediment bed at the height of 0.1 times of the pier width caused the maximum scour depth reduction around the pier. The results obtained by Moreno et al. (2015) revealed that the maximum reduction in scour depth at a complex bridge pier occurred when its pile cap was partly placed below the sediment bed. As the collar installation height increased above the sediment bed, more flow could pass under the collar. Therefore, the influence of the collar on reducing the scour around the pier was diminished (Tanaka and Yano 1967; Zarrati et al. 2004; Moncada-M et al. 2009).

Scour around two tandem piers has been investigated in several experimental and numerical studies (Hannah 1978; Selamoglu et al. 2014; Wang et al. 2016; Khaple et al. 2017b; Memar et al. 2018; Amini and Asadi Parto 2017; Keshavarzi et al. 2018). Ataie-Ashtiani and Beheshti (2006) demonstrated that scour depth around two tandem piers reached its maximum value at the center-to-center spacing of the piers of $s = 3D$, where D is the pier diameter. Numerical simulations were performed by Kim et al. (2014) to estimate the scour depth at two piers with the different center-to-center spacing of the piers. The results obtained from the above-cited studies indicated that the scour depth at two piers was highly influenced by the center-to-center spacing of the piers. Increasing the center-to-center spacing of the piers increased the scour depth, reaching the maximum values at $s = 3D - 3.5D$.

The experiments in this study were designed twofold. On the one hand, few studies have addressed the influence of collars on scour depth reduction at two tandem piers, for which the effect of collar height from the sediment bed has not been investigated (see Table 1). Thus, in the present study, this gap of knowledge was systematically studied by varying the width and height of collars from the sediment bed. Consequently, the best height of collars from the sediment bed, leading to the maximum scour depth reduction around the two tandem piers, was determined. On the other hand, in previous studies, the experiments have been conducted for a limited time (e.g., 7 h) without achieving the equilibrium scour depth. In this work, most of the experiments were performed for long durations (2–10 days),

reaching the equilibrium scour conditions. The effect of time on the performance of collars was examined.

Methods and materials

Dimensional analysis

The equilibrium depth of scour, d_{se} , at two cylindrical tandem piers protected by circular collars inserted in a wide rectangular channel with a movable bed consisting of uniform nonripple-forming quartz sand in clear-water conditions and uniform flow depends on the following: sediment features (submerged sediment density $\rho'_s = (\rho_s - \rho)$, sediment grain density ρ_s , median sediment grain size D_{50} , geometric standard deviation of the sediment grain size distribution σ_g), fluid features (density of fluid ρ , fluid kinematic viscosity ϑ), flow (mean upstream flow velocity U , upstream flow depth h), collar (countermeasure) features (width of collar w_c , collar height from sediment bed H_c , thickness of collar t_c), pier diameter D , width of channel B , mean threshold velocity U_c , which is defined as mean flow velocity for the onset of sediment movement (threshold condition), and the center-to-center spacing of piers s . Considering variables D , U and ρ as the repeaters and applying the Buckingham theorem lead to the following dimensionless relationship:

$$\frac{d_{se}}{D} = \varphi \left(\frac{U}{U_c}, \frac{\rho'_s}{\rho}, \frac{UD}{\vartheta}, \frac{s}{D}, \frac{h}{D}, \frac{B}{D}, \frac{w_c}{D}, \frac{H_c}{h}, \frac{t_c}{D}, \frac{D}{D_{50}}, \sigma_g \right) \quad (1)$$

where φ stands for the unknown function.

The effect of dimensionless parameters in Eq. (1) has been previously examined by researchers. To attain the equilibrium depth of scour in clear-water conditions, flow intensity (U/U_c) is adjusted near the threshold of sediment movement to a range of $0.9 \leq U/U_c \leq 1$. The uniform nonripple-forming quartz sand is characterized by $D_{50} \geq 0.6$ mm, $\rho_s \approx 2650$ (kg/m³) and $\sigma_g < 1.4$, as recommended by Dey et al. (1995). Moreover, the effect of sediment size (coarseness effect), flow depth (shallowness effect), viscosity and walls of the channel (wall effect) needs to be eliminated. In order to do so, the following conditions recommended by different researchers were applied to the experiments.

The effect of flow depth on local scouring was overlooked by using the criterion of Melville and Sutherland (1988), which is defined as $h/D \geq 2.6$. An upstream flow depth of $h = 0.165$ m was kept constant for all the experiments. The influence of sediment grain size on scour can be negligible if $D/D_{50} \approx 25$ –130 (Tafarojnoruz et al. 2010). In the case of wide channels, the wall effect on scour process associated with the existence of the piers in the channel was ignored considering $B/D \geq 10$ (Melville

Table 2 Conditions applied to the experiments and consequent interpretation

Dimensionless parameter	Theoretical range	Suggested by	Effect	Calculated values in this study	Resulted in the following conditions
D/D_{50}	$D/D_{50} \approx 25\text{--}130$	Tafarojnoruz et al. (2010)	Coarseness	35.4	The coarseness does not influence the scour depth
h/D	$h/D \geq 2.6$	Melville and Sutherland (1988)	Shalowness	2.6	Flow depth is not considered to be shallow (even though it is at the lowest margin for being shallow)
B/D	$B/D \geq 10$	Melville and Chiew (1999)	Wall	20.6	The scour depth is not influenced by the width of the channel
R_p	$R_p > 7000$	Monti (1994)	Viscosity	(22,680, 23,814)	Flow is fully turbulent
σ_g	$\sigma_g < 1.4$	Dey et al. (1995)	Uniform sediment	1.23	Sediment grains can be assumed uniform

and Chiew 1999). The pier Reynolds number $R_p = UD/\nu$ was greater than 7000 to avoid the impact of viscosity on the scour depth (Monti 1994). Table 2 also shows the conditions applied to the experiments.

Taking the experimental conditions of the study by Khaple et al. (2017b) into consideration, the center-to-center spacing of the piers was selected as three times of the pier diameter. The authors showed that the maximum depths of scour at two tandem piers could occur at the center-to-center spacing of the piers equal to three or two times of the pier diameter; for both spacings, the scour depth was approximately identical. The thickness of collar t_c was selected 3 mm to avoid influencing the scour development. Assuming the submerged sediment specific gravity (ρ'_s/ρ) almost invariant for sand and gravel (≈ 1.65) (Tafarojnoruz et al. 2012), Eq. (1) becomes:

$$\frac{d_{se}}{D} = \varphi \left(\frac{U}{U_c}, \frac{w_c}{D}, \frac{H_c}{h} \right) \quad (2)$$

In this study, the influences of collar height and the width of the collar on scour depth at two tandem piers with different flow intensities were examined. Table 3 presents the experimental conditions and dimensionless parameters.

Table 3 Experimental conditions and dimensionless parameters (Q discharge, D diameter of the pier, U mean upstream flow velocity, U/U_c flow intensity, U_c mean threshold velocity, h upstream flow depth, B width of the channel, D_{50} median sediment grain size, H_c

Experiment series	Q (l/s)	D (m)	U (m/s)	U/U_c	h (m)	B (m)	D_{50} (m)	H_c/h	w_c/D	s/D	R_p	F_r
I (reference)	77, 81	0.063	0.36	0.9, 0.95	0.165	1.3	0.00178	–	–	3	22,680 23,814	0.283 0.297
II	77	0.063	0.36	0.9	0.165	1.3	0.00178	0, –0.1	3	3	22,680	0.283
III	77	0.063	0.378	0.9	0.165	1.3	0.00178	0, –0.1	2	3	23,814	0.297
IV	81	0.063	0.378	0.95	0.165	1.3	0.00178	0, –0.1	2	3	23,814	0.297

Experimental installation

Laboratory experiments were performed in a straight part of a curved rectangular cross-section channel with 9 m length, 1.3 m width and 0.6 m depth at Laboratory of Hydraulic Constructions (LCH-EPFL), Lausanne, Switzerland. The channel included the experiment section (recess box) located 4 m downstream from the inlet of the channel with 0.25 m depth and 5 m length in the streamwise direction. The sediment utilized in this study was quartz sand of the median diameter $D_{50} = 1.78$ mm and the geometric standard deviation of the sediment grain size distribution $\sigma_g = 1.23$. This sediment is considered nonripple forming and non-cohesive. The model piers were provided using circular transparent PVC tubes with the diameter of 0.063 m and located at 7 m from the channel inlet, where a fully developed flow was established. The water was delivered to the channel by an automatically operated pump and the discharge was measured by an electromagnetic discharge meter. A gate that was positioned at the end of the channel regulated the water depth (h). The water and sediment bed levels were measured with a digital point gauge having the precision of 0.1 mm. To generate a uniform flow distribution, a metal net and a filter sponge were placed at the inlet of the channel. Periscopes were fixed inside the piers to read the time development of

collar height from the sediment bed, w_c width of the collar, s center-to-center spacing of the piers, R_p pier Reynolds number, F_r Froude number)

scour depth in front of the piers from the ruler papers glued to the piers. A Go Pro camera was installed on the wall of the channel under the water to take pictures and record videos of the scouring process around the piers. A 3D laser Baumer, OADM 1317480/S35A, mapped the topography of the scour holes around the piers at the end of the experiments.

The critical shear velocity u_c^* was initially determined through the method presented by Lança et al. (2015), which is $u_c^* = \sqrt{\Delta g D_{50} \tau_c^*} \approx 0.032$ and the critical shear stress is $\tau_c = \rho u_c^{*2}$. Parameter τ_c^* is the critical value of the shields parameter that is defined as: $\tau_c^* = 0.24/d^* + 0.055[1 - \exp(-d^{*1.05}/58)]$, where d^* is $\sqrt[3]{g\Delta D_{50}^3/\vartheta^2}$. The mean threshold velocity U_c was estimated using different relationships suggested by Shamov (1952) [cited in Dey (2014)], Melville and Sutherland (1988), Shepard et al. (2013) and Lança et al. (2015). Then, its value was determined by conducting some experiments without locating the piers and countermeasures in the channel. The results were in good agreement with the relationship recommended by Shamov (1952) [cited in Dey (2014)]. In the present work, most of the experiments were performed for a long duration (2–10 days). To stop the experiments, the criterion of Melville and Chiew (1999) was used. According to Melville and Chiew (1999), when the scour depth discrepancies during 24 h is not more than 5% of the pier diameter, the equilibrium phase is reached.

Configurations of experiments

For assessing the optimal height of collars from the sediment bed results in the minimum scour depth at the piers' front, the collars were positioned: (1) on the sediment bed $H_c = 0$ and (2) beneath the sediment bed at $H_c = -0.1h$ (in which h is upstream flow depth), under two different flow intensities of 0.9 (experiment series II and III) and 0.95 (experiment series IV) (see Table 3). It has to be clarified that, in the present work, the collars were not placed above the sediment bed. Given the outcomes presented by Tanaka and Yano (1967) and Zarrati et al. (2004), as the collars'

installation height above the sediment bed was increased, the flow could pass more easily under the collar. As a consequence, the protective effect of the collar on scour depth at the pier was reduced. Two different circular collars (made from PVC transparent sheets) of width $w_c = 2D, 3D$ (where D is the pier diameter) were employed. The schematic plan of two tandem piers equipped with the circular collars with different width is shown in Fig. 2. Figure 3 shows the configurations of two tandem piers without and with the collars.

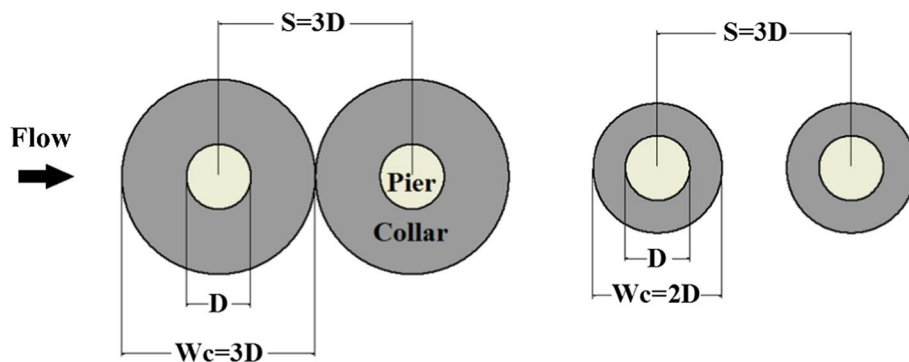
Results and discussion

Experimental observations

The results are shown in Table 4. Subscripts “ u ” and “ d ” refer to upstream and downstream piers. In the case of the experiments without collars (experiments A1 and A2), scour began at the front and sides of the piers, extended toward both downstream and upstream of them. By installing the collars around the piers, scour started from the downstream of the collars, then developed around the collars' edge and reached the piers' front after a time duration. Thus, the collars delayed the start of scour in front of the piers. The time from the beginning of the experiment to when the scour started at the piers' front is referred to as delay time and is shown by t_d in Table 4. Parameters t_{du} and t_{dd} indicate the delay time of scour at the upstream and downstream piers, respectively. In experiment C1, the rear of both collars was initially eroded. The scour began at the downstream pier's front after 1.5 h from the beginning of the experiment, while it reached the upstream pier's front later at $t_{du} = 2.5$ h. However, in the other cases (experiments C2, D1, D2), the delay time of scour at the upstream pier was greater than that at the downstream pier ($t_{du} > t_{dd}$) (see Table 4). This is due to the lower rate of scouring in experiment C1 than the other cases.

In the experiment series II, the broader collars $w_c = 3D$ caused maximum reduction in scour depth of about 100% at the collar height of $H_c = 0$ and the average of 82% at $H_c = -0.1h$ in front of the piers (at $t \approx 250$ min), where h stands for

Fig. 2 Schematic plan of two tandem piers equipped with collars (w_c width of the collar, D diameter of the pier, s center-to-center spacing of the piers)



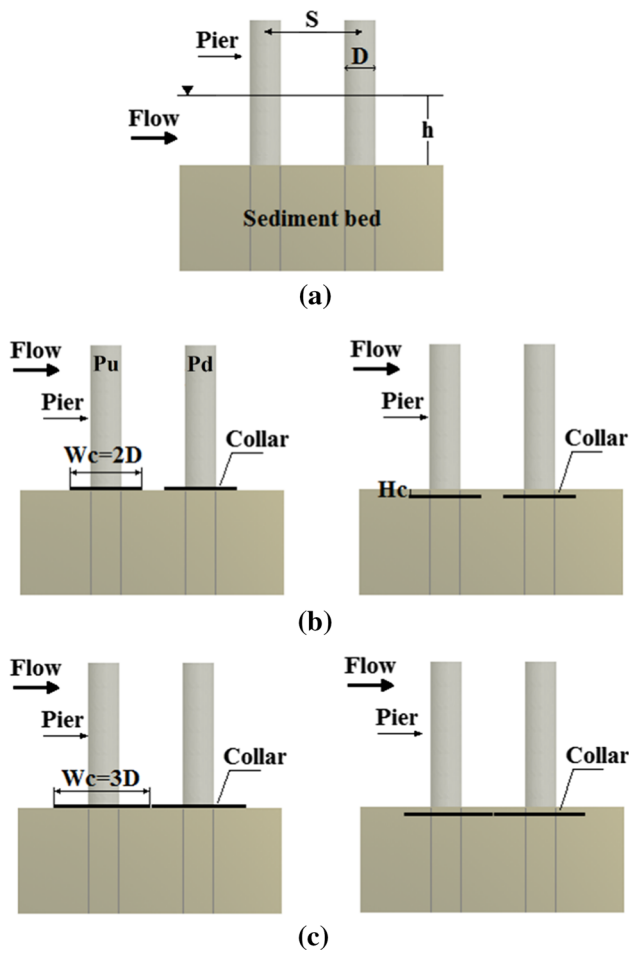


Fig. 3 Configurations of studied experiments: **a** two tandem piers, **b** two tandem piers equipped with collars of widths $w_c = 2D$, located on the sediment bed ($H_c = 0$) and beneath the sediment bed ($H_c = -0.1h$), **c** two tandem piers equipped with collars of widths $w_c = 3D$, located on the sediment bed ($H_c = 0$) and beneath the sediment bed ($H_c = -0.1h$) (s center-to-center spacing of the piers, D diameter of the pier, H_c collar height from the sediment bed, h upstream flow depth)

upstream flow depth. It was observed that approximately 5 min after the experiments began, sediments on the collars scoured. Collars covered the sediment bed around the piers and between them; therefore, scour occurred at the flank and downstream of collars with no upstream erosion (see Fig. 4).

Time development of scour depth in front of the two tandem piers (experiments A1 and A2) is represented in Fig. 5 on a logarithmic scale. The equilibrium depth of scour at upstream piers was on average 30% greater than their values for the downstream piers. The existence of the upstream pier led to flow velocity reduction toward the downstream pier. Thus, the power of downflow and horseshoe vortices around the downstream pier was weakened. In consequence, the rate of scouring at the upstream pier was higher than that at the downstream pier. Parameters P_u and P_d symbolize the upstream and downstream piers, respectively.

Influence of collar height on scour depth

Dimensionless time development of scour depth at two tandem piers equipped with the collars with width $w_c = 2D$ for different collar height can be compared, as shown in Fig. 6, with the coordinates of Oliveto and Hager (2002, 2005) and characterized as follows:

$$Z = \frac{d_s}{z_R}, \quad z_R = (hD^2)^{1/3} \tag{3}$$

$$T = \frac{t}{t_R}, \quad t_R = \frac{z_R}{\sigma^{1/3}(\Delta g D_{50})^{1/2}} \tag{4}$$

$$D^* = D_{proj} * K_{sp} * K_m \tag{5}$$

where $F_d = U/(\Delta g d_{50})^{1/2}$ is densimetric particle Froude number, D_{50} is median sediment size, $\Delta g = [(\rho_s - \rho)/\rho]g$, ρ is fluid density, ρ_s is sediment grain density, g is acceleration

Table 4 Dimensionless parameters, experiment duration (time of scour) t , delay time t_d , scour depth at the front of the piers d_s , extrapolated scour depth at the front of the piers at infinite time $d_{s(exp)}$

Series	Experiment	U/U_c	w_c/D	H_c/h	t (h)	t_{du} (h)	t_{dd} (h)	d_{su} (m)	d_{sd} (m)	$d_{su(exp)}$ (m)	$d_{sd(exp)}$ (m)
I (reference)	A1 ^a	0.9	–	–	62.5	–	–	0.105	0.081	0.116	0.088
	A2 ^a	0.95	–	–	120	–	–	0.129	0.096	0.145	0.106
II	B1	0.9	3	0	250	–	–	0	0	–	–
	B2	0.9	3	–0.1	240	–	–	0.0165	0.0165	–	–
III	C1 ^a	0.9	2	0	72	2.5	1.5	0.024	0.0135	0.03	0.025
	C2	0.9	2	–0.1	41	11	13	0.055	0.0315	0.103	0.043
IV	D1 ^a	0.95	2	0	144	2	3	0.106	0.065	0.122	0.08
	D2	0.95	2	–0.1	44	9	11.5	0.09	0.045	0.124	0.084

Subscripts u and d refer to the first and second piers, respectively

^aEquilibrium condition

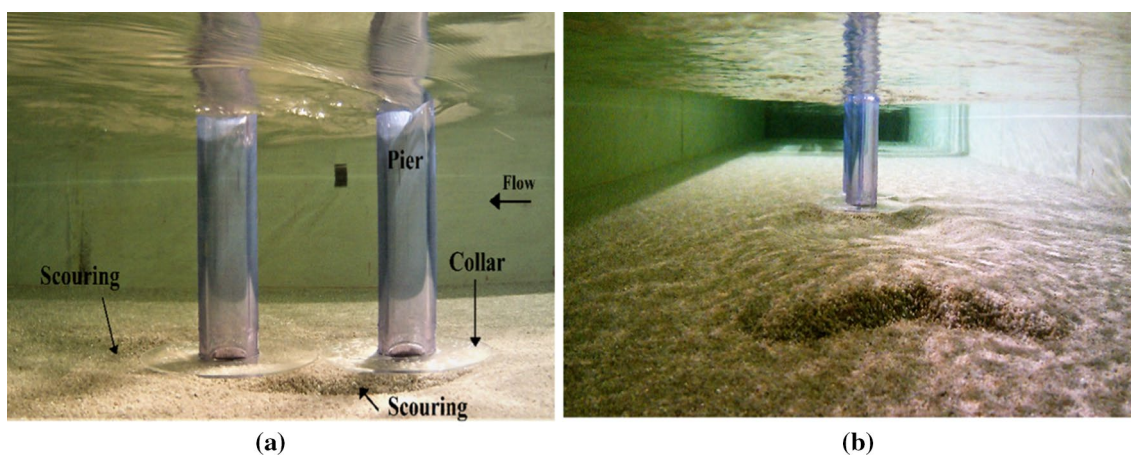


Fig. 4 The scour around two tandem piers equipped with collars of width $w_c = 3D$ located on the sediment bed: **a** side view and **b** view from downstream in the upstream direction ($t > 200$ h, under the water)

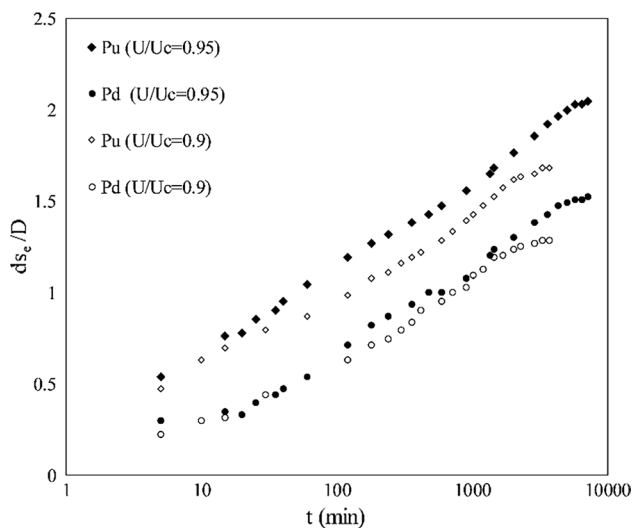


Fig. 5 The scour depth development at the front of two tandem piers at different flow intensities, in logarithmic scale (d_{se} equilibrium depth of scour, D diameter of the pier, t time of scour)

of gravity, Z is dimensionless scour depth, T is dimensionless time of scour, d_s is the maximum depth of scour, t is time of scour, σ_g is geometric standard deviation of the sediment grain size distribution and h is upstream flow depth. To consider the piers interaction effect on scour depth, the effective width of an equivalent full depth pier (D^*), recommended by FHWA (HEC-18), was replaced with the pier diameter. Thus, D_{proj} is the sum of the non-overlapping projected widths of the piers, K_{sp} is center-to-center spacing factor and K_m is the number of aligned rows factor (see Arneson et al. 2012).

Results indicated that locating the collars beneath the sediment bed increased delay time t_d compared to the case that the collars were set on the bed. However, greater scour depth

occurred at the front of the piers (see also Table 4). In the case of $H_c = -0.1h$, the obtained delay times were on average 4 and 5.5 times larger than the case of $H_c = 0$ at the upstream and downstream piers, respectively. After time t_d , the collars on the sediment bed can more efficiently slow down the scouring rates than the collars under the bed. This is proved by the slopes of the scour development curves in Fig. 6. Therefore, the optimal height of collars from the sediment bed, for which the maximum reduction of scour depth around the piers occurred, was $H_c = 0$ (on the original sediment bed).

Effect of time of scour on the collar’s effectiveness

As already mentioned, the dimensions of the scour hole around a bridge pier are increasing until the equilibrium scour condition is achieved. Conversely, some authors claim that the scour process may carry on even if the scour topography seems to attain an equilibrium state (Oliveto and Hager 2002, 2005). Given these points, it is essential to assess the effect of collars on scour depth around the piers in the equilibrium condition. Additionally, assuming that the equilibrium phase is attained asymptotically (Chabert and Engeldinger 1956; Etema 1980), the measured depth of scour at the end of the experiments was extrapolated to the infinite time ($t = \infty$) using the equation recommended by Lança et al. (2010). The extrapolated depth of scour is presented by $d_{s(exp)}$ in Table 4. The values of scour depth reduction R are calculated using Eq. (6):

$$R(\%) = \frac{d_{s0} - d_s}{d_{s0}} * 100 \tag{6}$$

where subscript 0 indicates the experiments without collars. In Table 5, the scour depth reduction values for different times of the experiments and for the infinite time (for the

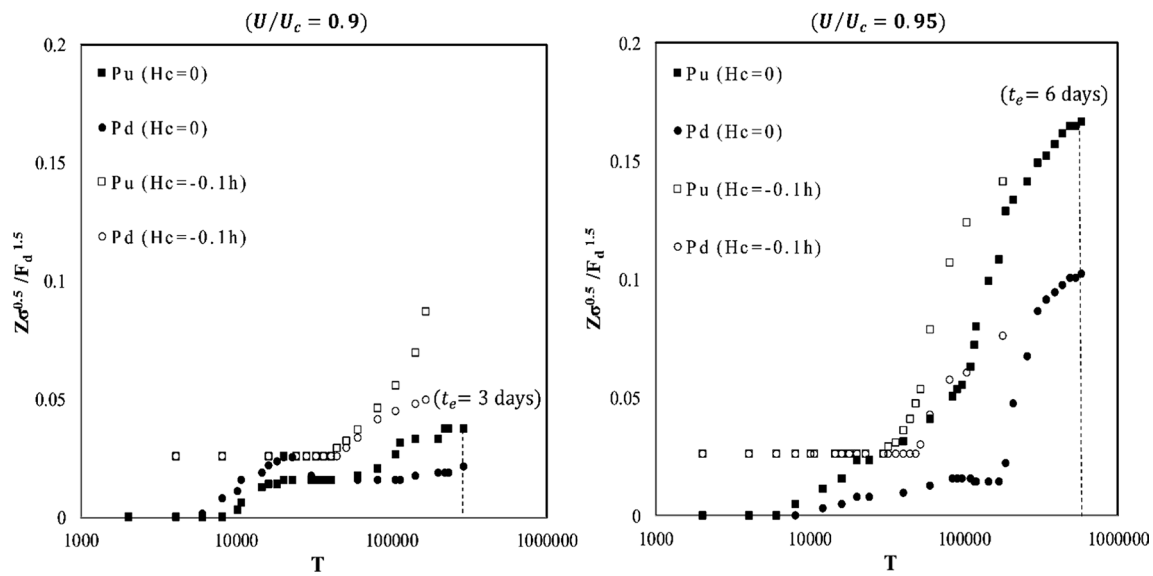


Fig. 6 Dimensionless development of the scour depths at the front of two tandem piers protected by collars for collar heights of $H_c = 0$ and $H_c = -0.1h$, at different flow intensities, with the coordinates of Oliveto and Hager (2002, 2005), in logarithmic scale (Z dimension-

less scour depth, T dimensionless time of scour, σ_g geometric standard deviation of the sediment grain size distribution, F_d densimetric particle Froude number, h upstream flow depth (also see Fig. 3b)

Table 5 Percent reduction in scour depth at different times t , at the front of the first pier R_u and the second pier R_d (H_c/h collar height from sediment bed to the upstream flow depth, U/U_c flow intensity)

Series	Experiment	H_c/h	U/U_c	R_u (%)			R_d (%)		
				$t = 24$ h	$t = 40$ h	$t = \infty^a$	$t = 24$ h	$t = 40$ h	$t = \infty$
II	C1	0	0.9	83.3	82	74.13	86.6	86.5	71.5
	C2	-0.1	0.9	64.5	52	11.2	63.3	63	51.13
IV	D1	0	0.95	67	34	16	87	88	24.5
	D2	-0.1	0.95	28.3	15.1	14.4	40	43	20.1

^aInfinite time

extrapolated scour depths) are given. Parameters R_u and R_d represent the scour depth reduction in front of the upstream and downstream piers. The results showed that the effectiveness of collars was a time-dependent parameter. Comparing the scour depth reduction at both collar heights revealed that, when the collars were placed on the bed, the maximum efficiency for them was obtained.

As can be observed in Fig. 7, when the collars were installed on the bed (experiments C1 and D1), the effect of the collar was decreased over time at the upstream pier. At the downstream pier, the scouring process was influenced by the upstream sediment transport. The moving sediment grains from upstream were continuously entering and leaving the scour hole around the downstream pier until the region between the piers was flattened. The minimum reduction in scour depth was related to the final state (extrapolated depth of scour). For $H_c = -0.1h$, the scour depth reduction was depicted after the delay time t_d .

Additionally, in experiments C1 and D1, as the flow intensity enhanced from 0.9 to 0.95, the maximum

reduction in scour depth was decreased from the average of 70–20% at the piers. The equilibrium time of scour under the flow intensity of 0.95 (experiment D1) was nearly two times of its value under the flow intensity of 0.9 (experiment C1). As mentioned before, after the scour reached the piers’ front, the rate of scour around the piers under the flow intensity of 0.95 was higher than under the flow intensity of 0.9, as evident by the slopes of scouring curves in Fig. 6. According to Melville and Chiew (1999) under clear-water conditions, scour depth enhances with flow intensity (which is determined as the relative mean flow velocity (U) to the mean threshold velocity (U_c)), reaching a maximum amount at the flow intensity equal to 1. Generally, increasing the flow intensity increases the erosive effect of the flowing water, as the bed-shear stress enhances. As the consequence, the scouring rate around the piers enhances. The process of sediment grains erosion is consistent with prevailing bed-shear stress, which can be defined from the measured velocity profile (Houwing and Van Rijn 1998).

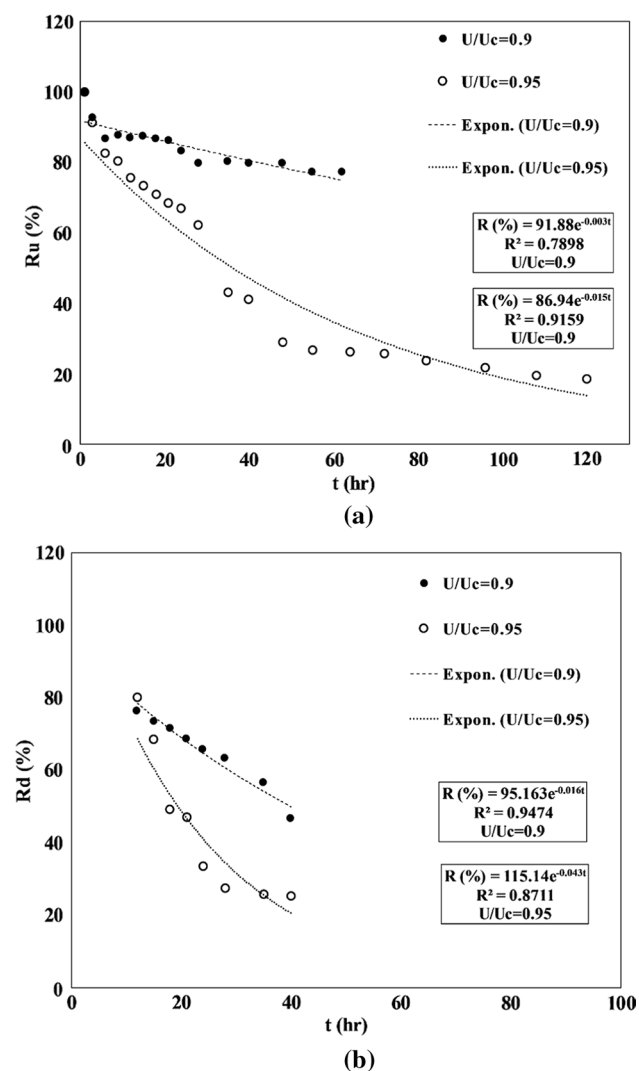


Fig. 7 Reduction in scour depth over time t (experiments C1 and D1): **a** at the front of the first pier R_u , **b** at the front of the second pier R_d , at different flow intensities U/U_c

Given the results explained above, at the piers protected by collars, the flow intensity makes a significant contribution to scour phenomena at the pier's site. The results are in line with those found by Karimaei Tabarestani and Zarrati (2019). The authors indicated that the flow intensity was a

dominant variable affecting the effectiveness of the collar in scour depth reduction around the pier. In Fig. 6, the equilibrium times are shown by the dotted lines.

Figure 8 shows the column diagram of the scour depth reduction at different times of the experiments. The eroded sediment beds at the end of experiments C1 and D1 are demonstrated in Fig. 9. The equilibrium depth of scour in front of two tandem piers protected by the collars is demonstrated with contour lines in Fig. 10. Recall that experiments C1 and D1 were performed until the equilibrium scour condition was achieved.

Conclusions

In this experimental work, the effect of the collar width and collar height from the sediment bed on the reduction in scour depths at two tandem piers was investigated. The following conclusions were made:

1. The optimal height of the collars from the bed, for which the maximum scour reductions around the piers was obtained, was the height of the initial sediment bed (collars situated on the sediment bed).
2. The flow intensity significantly influenced the scour depth at the piers equipped with collars. Generally, under clear-water conditions, by increasing the flow intensity, the scour depth at piers enhances. Herein, reducing the flow intensity from 0.95 to 0.9 increased the maximum reduction in scour depth from the average of 20–70% (for the collars placed on the bed).
3. For the collars set underneath the sediment bed, scour reached the piers' front at the much longer time than the condition, in which the collars were on the sediment bed. However, greater scour depth occurred in front of the piers. To put it another way, the delay time (the time from starting the experiment to when the scour started at the front of the piers) was increased for the average of 4 and 5.5 times at the upstream and downstream piers, correspondingly.
4. The collar's performance depended on time and decreased over time.

Fig. 8 Column diagram of the scour depth reduction for different time durations of the experiments at different flow intensities U/U_c (R_u reduction in scour depth for the first pier, R_d reduction in scour depth for the second pier, t time of scour)

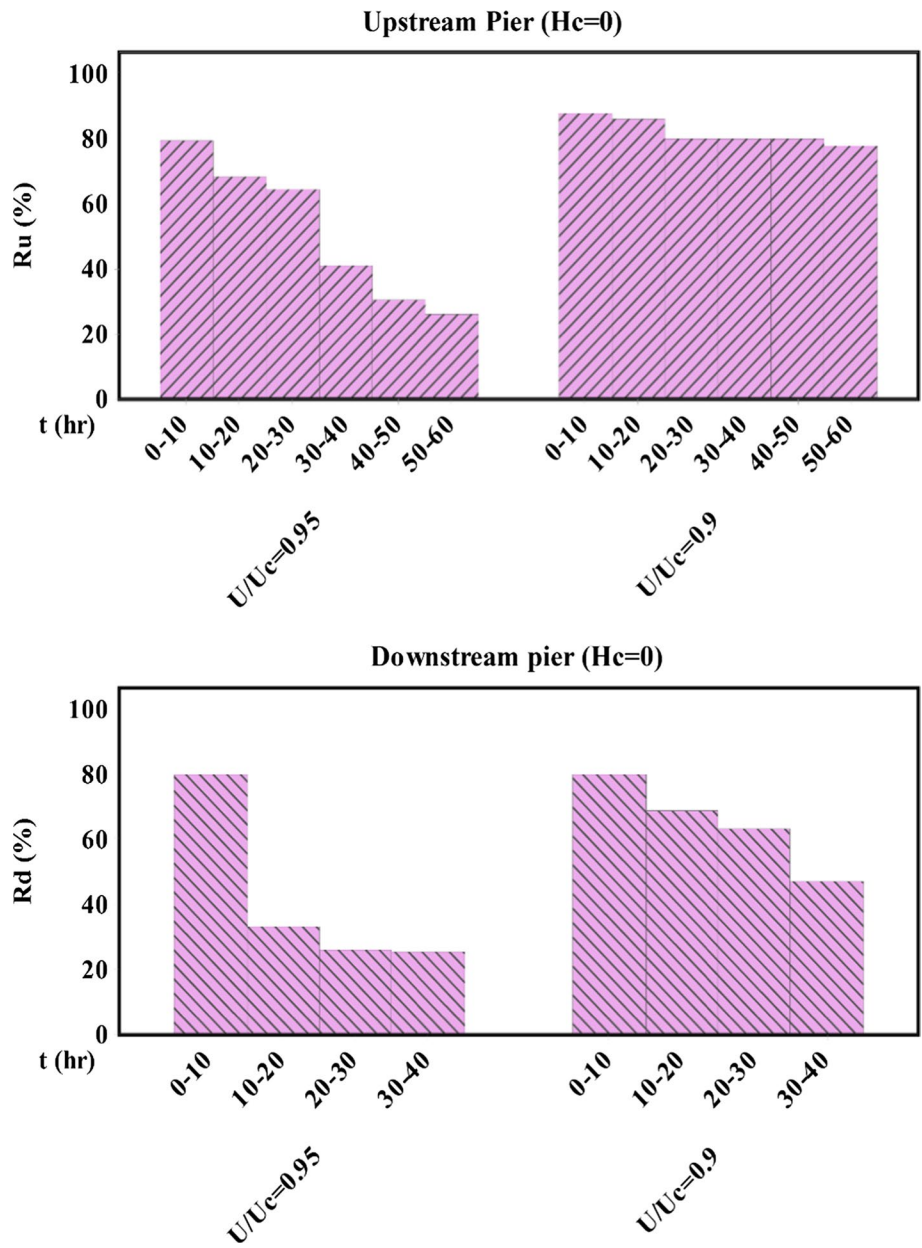


Fig. 9 Eroded sediment bed at the end of experiments C1 and D1 at different flow intensities (for collar width $w_c = 2D$, and collar height $H_c = 0$)

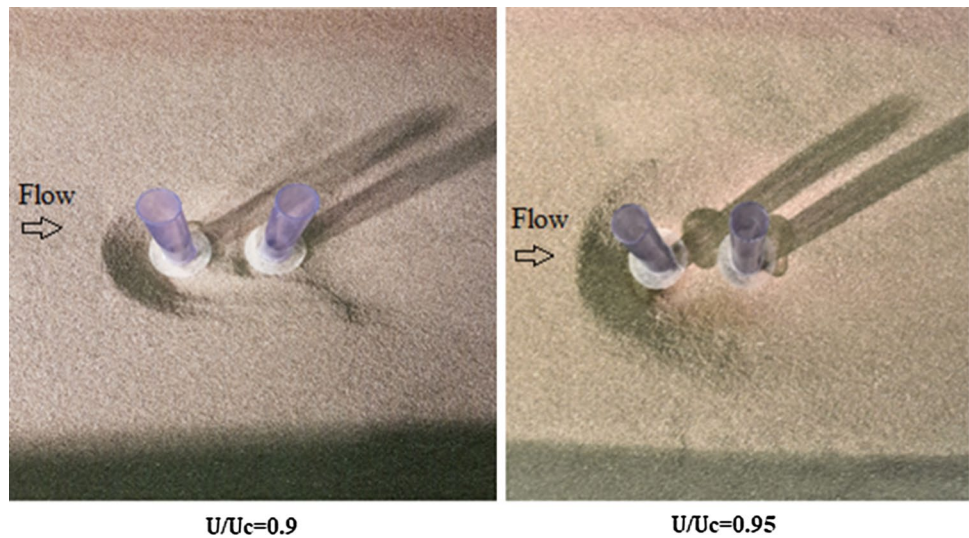
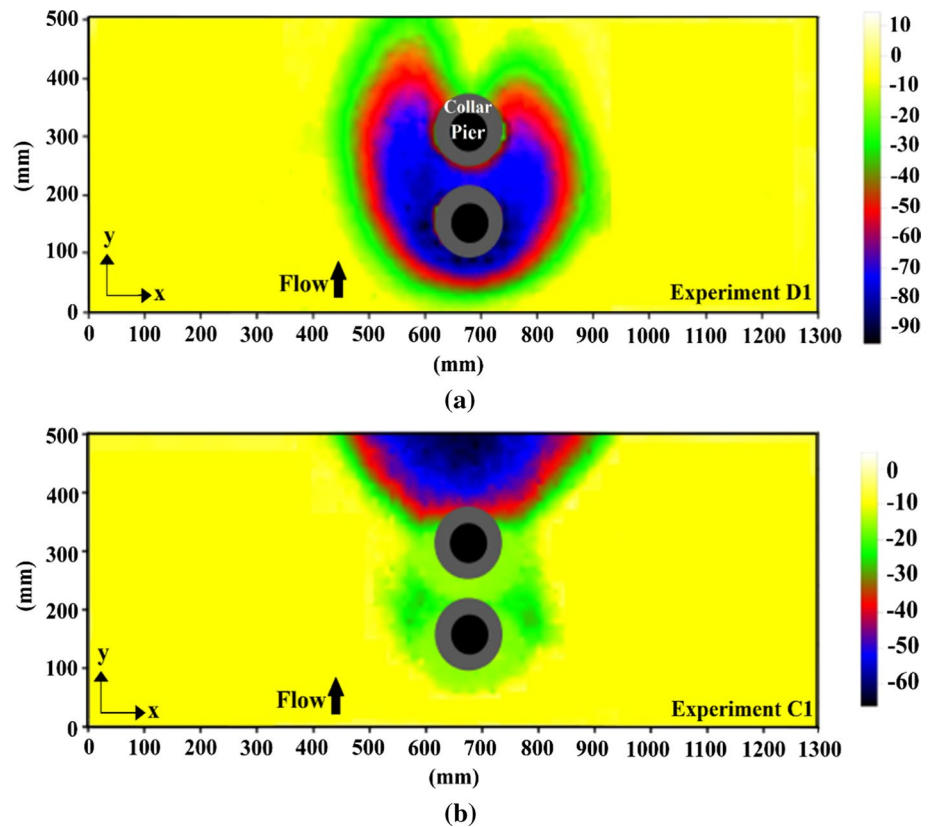


Fig. 10 Contour lines of scour at tandem piers equipped with collars on the sediment bed ($H_c = 0$) at different flow intensities, at the equilibrium time: **a** experiment D1, **b** experiment C1



Acknowledgements This experimental research was conducted at Laboratory of Hydraulic Constructions (LCH-EPFL), Lausanne, Switzerland, which supported the project financially as well.

Compliance with ethical standards

Conflict of interest The authors declare that they have no conflict of interest.

References

- Amini A, Asadi Parto A (2017) 3D numerical simulation of flow field around twin piles. *Acta Geophys* 65(6):1243–1251. <https://doi.org/10.1007/s11600-017-0094-x>
- Arneson PF, Zevenbergen LA, Lagasse LW (2012) Evaluating scour at bridges. Hydraulic engineering circular no. 18 (HEC-18) (report no. FHWA NHI 01-001). Federal Highway Administration, Washington, DC

- Ataie-Ashtiani B, Beheshti AA (2006) Experimental investigation of clear-water local scour at pile groups. *J Hydraul Eng* 132(10):1100–1104. [https://doi.org/10.1061/\(ASCE\)0733-9429\(2006\)132:10\(1100\)](https://doi.org/10.1061/(ASCE)0733-9429(2006)132:10(1100))
- Chabert J, Engeldinger P (1956) Study of scour around bridge piers. Report prepared for the Laboratoire National d'Hydraulique
- Chen SC, Tfwala S, Wu TY, Chan HC, Chou HT (2018) A hooked-collar for bridge piers protection: flow fields and scour. *Water* 10(9):1251. <https://doi.org/10.3390/w10091251>
- Chiew YM (1984) Local scour at bridge piers. Doctoral dissertation, University of Auckland
- Dey S (1997a) Local scour at piers, part I: a review of developments of research. *Int J Sediment Res* 12(2):23–46
- Dey S (1997b) Local scour at piers, part II: bibliography. *Int J Sediment Res* 12(2):47–57
- Dey S (2014) *Fluvial hydrodynamics*. Springer, Berlin
- Dey S, Bose SK, Sastry GLN (1995) Clear water scour at circular piers: a model. *J Hydraul Eng* 121:869–876. [https://doi.org/10.1061/\(ASCE\)0733-9429\(1995\)121:12\(869\)](https://doi.org/10.1061/(ASCE)0733-9429(1995)121:12(869))
- Ettema R (1980) Scour at bridge piers. Report no. 216. University of Auckland, Auckland, New Zealand
- Ettema R, Nakato T, Muste MVI (2006) An illustrated guide for monitoring and protecting bridge waterways against scour (No. Project TR-515). IIHR-Hydroscience & Engineering, University of Iowa
- Guo J, Suaznabar O, Shan H, Shen J (2012) Pier scour in clear-water conditions with non-uniform bed materials (No. FHWA-HRT-12-022). Turner-Fairbank Highway Research Center, McLean
- Hannah CR (1978) Scour at pile groups. Report no. 78-3. Canterbury University, Canterbury, New Zealand
- Heidarpour M, Afzalimehr H, Izadinia E (2010) Reduction of local scour around bridge pier groups using collars. *Int J Sediment Res* 25(4):411–422. [https://doi.org/10.1016/S1001-6279\(11\)60008-5](https://doi.org/10.1016/S1001-6279(11)60008-5)
- Houwing EJ, Van Rijn LC (1998) In situ erosion flume (ISEF): determination of bed-shear stress and erosion of a kaolinite bed. *J Sea Res* 39(3–4):243–253
- Johnson PA, Hey RD, Brown ER, Rosgen DL (2002) Stream restoration in the vicinity of bridges. *J Am Water Resour Assoc* 38(1):55–67. <https://doi.org/10.1111/j.1752-1688.2002.tb01534.x>
- Karimaei Tabarestani M, Zarrati AR (2019) Local scour depth at a bridge pier protected by a collar in steady and unsteady flow. In: *Proceedings of the Institution of Civil Engineers—water management*. Thomas Telford Ltd, London, pp 1–11. <https://doi.org/10.1680/jwama.18.00061>
- Keshavarzi A, Shrestha CK, Melville BW, Khabbaz H, Ranjbar-Zahedani M, Ball J (2018) Estimation of maximum scour depths at upstream of front and rear piers for two tandem circular columns. *Environ Fluid Mech* 18(2):537–550. <https://doi.org/10.1007/s10652-017-9572-6>
- Khaple S, Hanmaiahgari PR, Gaudio R, Dey S (2017a) Splitter plate as a flow-altering pier scour countermeasure. *Acta Geophys* 65(5):957–975. <https://doi.org/10.1007/s11600-017-0084-z>
- Khaple S, Hanmaiahgari PR, Gaudio R, Dey S (2017b) Interference of an upstream pier on local scour at downstream piers. *Acta Geophys* 65(1):29–46. <https://doi.org/10.1007/s11600-017-0004-2>
- Khodashenas SR, Shariati H, Esmaeli K (2018) Comparison between the circular and square collar in reduction of local scouring around bridge piers. In: *E3S web of conferences*. EDP sciences, vol 40, p 03002
- Kim HS, Nabi M, Kimura I, Shimizu Y (2014) Numerical investigation of local scour at two adjacent cylinders. *Adv Water Resour* 70:131–147. <https://doi.org/10.1016/j.advwatres.2014.04.018>
- Kumar V, Raju KGR, Vittal N (1999) Reduction of local scour around bridge piers using slots and collars. *J Hydraul Eng* 125(12):1302–1305. [https://doi.org/10.1061/\(ASCE\)0733-9429\(1999\)125:12\(1302\)](https://doi.org/10.1061/(ASCE)0733-9429(1999)125:12(1302))
- Lança R, Fael C, Cardoso A (2010) Assessing equilibrium clear water scour around single cylindrical piers. In: *Proceedings of the international conference on fluvial hydraulic (river flow)*, Braunschweig, Germany, September 8–10
- Lança R, Fael C, Maia R, Pêgo JP, Cardoso AH (2013) Clear-water scour at pile groups. *J Hydraul Eng* 139(10):1089–1098. [https://doi.org/10.1061/\(ASCE\)HY.1943-7900.0000770](https://doi.org/10.1061/(ASCE)HY.1943-7900.0000770)
- Lança RMM, Simarro G, Fael CMS, Cardoso AH (2015) Effect of viscosity on the equilibrium scour depth at single cylindrical piers. *J Hydraul Eng* 142(3):06015022. [https://doi.org/10.1061/\(ASCE\)HY.1943-7900.0001102](https://doi.org/10.1061/(ASCE)HY.1943-7900.0001102)
- Masjedi A, Bejestan MS, Esfandi A (2010) Experimental study on local scour around single oblong pier fitted with a collar in a 180 degree channel bend. *Int J Sediment Res* 25(3):304–312. [https://doi.org/10.1016/S1001-6279\(10\)60047-9](https://doi.org/10.1016/S1001-6279(10)60047-9)
- Melville BW (1984) Live-bed scour at bridge piers. *J Hydraul Eng* 110(9):1234–1247. [https://doi.org/10.1061/\(ASCE\)0733-9429\(1984\)110:9\(1234\)](https://doi.org/10.1061/(ASCE)0733-9429(1984)110:9(1234))
- Melville BW, Chiew YM (1999) Time scale for local scour at bridge piers. *J Hydraul Eng* 114(10):1210–1226. [https://doi.org/10.1061/\(ASCE\)0733-9429\(1999\)125:1\(59\)](https://doi.org/10.1061/(ASCE)0733-9429(1999)125:1(59))
- Melville BW, Sutherland AJ (1988) Design method for local scour at bridge piers. *J Hydraul Eng* 114(10):1210–1226. [https://doi.org/10.1061/\(ASCE\)0733-9429\(1988\)114:10\(1210\)](https://doi.org/10.1061/(ASCE)0733-9429(1988)114:10(1210))
- Memar S, Zounemat-Kermani M, Beheshti A, De Cesare G, Schleiss AJ (2018) Investigation of local scour around tandem piers for different skew-angles. In: *International conference on fluvial hydraulics (river flow)*, Lyon-Villerurbanne, France, September 5–8
- Moncada-M AT, Aguirre-Pe J, Bolivar JC, Flores EJ (2009) Scour protection of circular bridge piers with collars and slots. *J Hydraul Res* 47(1):119–126. <https://doi.org/10.3826/jhr.2009.3244>
- Monti R (1994) Indagine sperimentale delle caratteristiche fluidodinamiche del campo di moto intorno ad una pila circolare. Tesi di Dottorato di Ricerca, Politecnico di Milano, Milan, Italy (**in Italian**)
- Moreno M, Maia R, Couto L (2015) Effects of relative column width and pile-cap elevation on local scour depth around complex piers. *J Hydraul Eng* 142(2):04015051. [https://doi.org/10.1061/\(ASCE\)HY.1943-7900.0001080](https://doi.org/10.1061/(ASCE)HY.1943-7900.0001080)
- Oliveto G, Hager WH (2002) temporal evolution of clear-water pier and abutment scour. *J Hydraul Eng* 128(9):811–820. [https://doi.org/10.1061/\(ASCE\)0733-9429\(2002\)128:9\(811\)](https://doi.org/10.1061/(ASCE)0733-9429(2002)128:9(811))
- Oliveto G, Hager WH (2005) Further results to time-dependent local scour at bridge elements. *J Hydraul Eng* 131(2):97–105. [https://doi.org/10.1061/\(ASCE\)0733-9429\(2005\)131:2\(97\)](https://doi.org/10.1061/(ASCE)0733-9429(2005)131:2(97))
- Pang ALJ, Skote M, Lim SY, Gullman-Strand J, Morgan N (2016) A numerical approach for determining equilibrium scour depth around a mono-pile due to steady currents. *Appl Ocean Res* 57:114–124. <https://doi.org/10.1016/j.apor.2016.02.010>
- Raudkivi AJ (1986) Functional trends of scour at bridge piers. *J Hydraul Eng* 112(1):1–13. [https://doi.org/10.1061/\(ASCE\)0733-9429\(1986\)112:1\(1\)](https://doi.org/10.1061/(ASCE)0733-9429(1986)112:1(1))
- Selamoglu M, Yanmaz AM, Koken M (2014) Temporal variation of scouring topography around dual bridge piers. In: *Proceedings of the seventh international conference on scour and erosion*, Perth, Western Australia
- Shen HW, Schneider VR, Karaki SS (1966) *Mechanics of local scour*. Report no. CER66HWS10. Colorado State University, Fort Collins, CO
- Sheppard DM, Miller W Jr (2006) Live-bed local pier scour experiments. *J Hydraul Eng* 132(7):635–642
- Sheppard DM, Melville B, Demir H (2013) Evaluation of existing equations for local scour at bridge piers. *J Hydraul Eng* 140(1):14–23. [https://doi.org/10.1061/\(ASCE\)HY.1943-7900.0000800](https://doi.org/10.1061/(ASCE)HY.1943-7900.0000800)

- Tafarojnoruz A, Gaudio R, Grimaldi C, Calomino F (2010) Required conditions to achieve the maximum local scour depth at a circular pier. In: Proceeding XXXII Convegno Nazionale di Idraulica e Costruzioni Idrauliche, 14–17 September, Palermo, Italy, Farina, Palermo
- Tafarojnoruz A, Gaudio R, Calomino F (2012) Evaluation of flow-altering countermeasures against bridge pier scour. *J Hydraul Eng* 138(3):297–305. [https://doi.org/10.1061/\(ASCE\)HY.1943-7900.0000512](https://doi.org/10.1061/(ASCE)HY.1943-7900.0000512)
- Tanaka S, Yano M (1967) Local scour around a circular cylinder. In: Proceeding of 12th IAHR congress. International Association for Hydraulic Research, Delft, Netherlands
- Wang H, Tang H, Liu Q, Wang Y (2016) Local scouring around twin bridge piers in open-channel flows. *J Hydraul Eng* 142(9):06016008. [https://doi.org/10.1061/\(ASCE\)HY.1943-7900.0001154](https://doi.org/10.1061/(ASCE)HY.1943-7900.0001154)
- Zarrati AR, Gholami H, Mashahir MB (2004) Application of collar to control scouring around rectangular bridge piers. *J Hydraul Res* 42(1):97–103. <https://doi.org/10.1080/00221686.2004.9641188>
- Zarrati AR, Nazariha M, Mashahir MB (2006) Reduction of local scour in the vicinity of bridge pier groups using collars and riprap. *J Hydraul Eng* 132(2):154–162. [https://doi.org/10.1061/\(ASCE\)0733-9429\(2006\)132:2\(154\)](https://doi.org/10.1061/(ASCE)0733-9429(2006)132:2(154))
- Zokaei M, Zarrati AR, Salamatian SA, Tabarestani MK (2013) Study on scouring around bridge piers protected by collar using low density sediment. *Int J Civ Eng* 11(3A):199–205
- Zounemat-Kermani M, Beheshti AA, Ataie-Ashtiani B, Sabbagh-Yazdi SR (2009) Estimation of current-induced scour depth around pile groups using neural network and adaptive neuro-fuzzy inference system. *Appl Soft Comput* 9(2):746–755. <https://doi.org/10.1016/j.asoc.2008.09.006>